JEE Journal of Ecological Engineering

Journal of Ecological Engineering, 2025, 26(12), 449–464
https://doi.org/10.12911/22998993/209091
ISSN 2299–8993, License CC-BY 4.0

Received: 2025.07.21
Accepted: 2025.09.01
Published: 2025.10.01

Comparative evaluation of silver oxide nanoparticles and spirulina platensis for the remediation of real industrial wastewater

Ali Y. Alwan[1,2], Naser Jafari[1], Rana Ibrahim Khaleel[3*]

[1] Department of Biology, Faculty of Basic Sciences, University of Mazandaran, Babolsar, Iran
[2] College of Applied Sciences, University of Samarra, Iraq
[3] Department of Architecture, College of Engineering, University of Samarra, Iraq
* Corresponding author's e-mail: rana.ibrahim@uosamarra.edu.iq

ABSTRACT

This study investigates the comparative efficiency of silver oxide (Ag_2O) nanoparticles and the microalga *Spirulina platensis* in the remediation of real industrial wastewater. Ag_2O nanoparticles were synthesized via chemical precipitation and characterized using X-ray diffraction (XRD), Fourier-transform infrared spectroscopy FTIR, scanning electron microscopy (SEM), and atomic force microscopy (AFM). SEM analysis revealed that the nanoparticles had a mean particle size of approximately 47 nm, while AFM confirmed the presence of moderately aggregated structures. Spirulina platensis was identified through microscopic examination and used as a biological treatment agent. The treatment performance of both materials was assessed through key physicochemical parameters such as total dissolved solids (TDS), turbidity, chemical oxygen demand (COD), nitrate, phosphate, and heavy metals. Ag_20 nanoparticles achieved high removal efficiencies, including 92% for lead (Pb), 88% for turbidity, and 85% for COD. In comparison, *Spirulina platensis* demonstrated effective nutrient reduction, with 75% phosphate and 70% nitrate removal. Although both treatments were effective, AgO nanoparticles showed superior performance in eliminating heavy metals and persistent chemical contaminants, while *Spirulina* excelled in nutrient reduction. These findings suggest the potential of integrating nanotechnology and phycoremediation for sustainable wastewater treatment.

Keywords: industrial wastewater treatment, silver oxide nanoparticles, *Spirulina platensis*, bioremediation.

INTRODUCTION

Industrial effluents represent a persistent challenge in modern environmental management due to their complex composition, including high levels of toxic organics, heavy metals, and refractory compounds. These pollutants are not only difficult to degrade but also pose immediate and long-term threats to aquatic ecosystems and human well-being when discharged untreated. Despite the evolution of conventional treatment technologies, such as coagulation–flocculation and activated sludge systems, many industrial discharges remain inadequately treated, revealing the limitations of these approaches in handling diverse and highly concentrated contaminants (Benedetti et al., 2021; Kumar et al., 2021). In response, researchers have turned toward novel and sustainable alternatives capable of improving treatment outcomes. Among these, nanomaterials – particularly silver oxide nanoparticles (Ag_2O NPs) – have emerged as highly efficient agents due to their pronounced oxidative potential and reactivity. These nanoparticles have shown remarkable performance in degrading organic dyes, reducing chemical oxygen demand (COD), and removing metal ions from complex wastewater matrices (Chakraborty et al., 2022; Gungure et al., 2024). Their rapid kinetics and catalytic surface properties make them promising for high-load industrial applications. In parallel, biological approaches have gained attention as eco-friendly alternatives. The cyanobacterium *Spirulina platensis* has been

recognized for its biosorptive capabilities, especially in binding and accumulating heavy metals and organic pollutants. As a cost-effective and biodegradable agent, Spirulina offers dual advantages in environmental remediation and biomass valorization (Diaconu et al., 2023; Bhukal et al., 2022). Furthermore, *Spirulina*-based materials have been developed into functional biosorbents with enhanced removal capacity for various micro-contaminants (Pedrosa et al., 2022). Despite the advancements in both fields, comparative assessments under unified experimental conditions remain scarce. This study addresses this gap by evaluating and comparing the treatment efficiency of Ag_2O nanoparticles and *Spirulina platensis* in removing COD, turbidity, and selected heavy metals from real industrial wastewater. The findings aim to highlight not only the efficacy of each method but also their practicality and sustainability in large-scale applications.

MATERIALS AND METHODS

Chemicals and reagents

These reagents and chemicals were used without further purification: $AgNO_3$ was from Germany, while Ethanol and Rifampicin were from CDH and Wellona Pharma, India. Besides, Sodium Carbonate and Sodium Hydroxide were from Sigma Aldrich, Germany, and CDH, India. Also, Sodium Carbonate and Sodium Hydroxide from Sigma Aldrich, Germany, and CDH, India. A few of the other major chemicals employed in the research are Ascorbic Acid, Ethylene Glycol, and other salts such as NaCl, $MgCl_2$, and H_3PO_4, which were obtained from firms such as BDH, Riedeldehaen, and Merck respectively.

Characterization

D8 Bruker Discover Series 2 diffractometer was used to perform X-ray powder diffraction studies, with a Cu Kα radiation source (λ = 1.5406 Å). X-ray diffraction patterns were gathered using a step size of 0.04° and a step period of 0.2 s per point throughout a 2θ range of 20–80°. The crystalline phases were determined from the JCPDS database. Fourier transform infrared spectroscopy (FT-IR) was performed on a Perkin-Elmer 1000 FT-IR spectrophotometer and thermogravimetric analysis on a Perkin-Elmer thermogravimetric analyzer. Scanning electron microscopy (SEM) was performed to determine the shape and size of the samples in a low-vacuum SEM JEOL JSM-6610LV (20 kV). The isolated cyanobacteria species were identified in the study using a light microscope equipped with a photographic camera(Waterbury, 2006). Some laboratory tests were also done to assess the quality of water samples before and after treatment with cyanobacteria. The tests were started with some physical parameters: electrical conductivity and suspended solids in the water. The second group of tests included chemical parameters like COD, phosphate (PO_4), sulfate (SO_4), acidity (pH), and the presence of nitrite (NO_2), nitrate (NO_3), and heavy metals. According to Standard Methods for the Examination of Water and Wastewater (SMEWW) 23rd edition 2017(APHA et al., 2017).

Preparation of Ag_2O

Silver oxide nanoparticles (Ag_2O NPs) were prepared by using an eco-friendly green synthesis process. Initially, 0.1 M silver nitrate ($AgNO_3$) was dissolved in 50 mL of deionized water under stirred conditions until it was completely dissolved. To the $AgNO_3$ solution, 10 mL of ascorbic acid solution having a concentration of 0.001 M was added dropwise as a reducing agent.The pH of the solution was subsequently changed from 6.7 to 11 by adding 0.2 M increments of sodium hydroxide (NaOH) while stirring. This facilitated the reduction of silver ions (Ag^+) to metallic silver (Ag^0), which was indicated by the color change from colorless to brown. The brown solution produced was allowed to precipitate, which was then annealed at 80 °C for 2 hours to achieve silver oxide nanopowder (Chen, Chiang and Huang, 2016; Fayyadh and Jaduaa Alzubaidy, 2021). The annealed product was ground again to fine powder for the sake of achieving a uniform powder, which was further subjected to characterization to explore its physicochemical properties and potential application.

Preparation of cyanobacteria

Selective medium BG11 with full nutrient composition provides all the nutritional needs of cyanobacteria(Hirata et al., 2000; Yashavanth et al., 2021). Selective agricultural medium type ASM-1 was also utilized for cyanobacterial isolation and cultivation (Gallon et al.,

1978) and utilized in numerous previous studies regarding cyanobacteria. The ASM-1 medium consists of the substances listed in Table 2, with their respective units of measurement indicated in micromoles per liter (μmol/L). For preparing the solid medium, agar was added to the liquid medium at a ratio of 1 gram per 100 mL, and the mixture was sterilized again. It was then cooled to below 50 °C and poured into Petri dishes under sterile environmental conditions near a Bunsen burner. Once cooled and solidified, the dishes were incubated at 37 °C for 24 to 48 hours to ensure they were free of microbial contamination, before being transferred to the refrigerator until needed.

The said chemicals were dissolved in distilled water at the given concentrations and stirred all the time by a magnetic stirrer on a heat plate for maximum dissolution and homogeneity of the medium components. pH was maintained between 7.6 and 7.8 using sodium bicarbonate ($NaHCO_3$) or diluted hydrochloric acid (HCl) of 0.1 M concentration. The solution was then divided into 100 mL aliquots in 250 mL flasks and sealed with cotton plugged with medical gauze and silicone. The flasks were autoclaved at 121 °C and 15 psi for 15 minutes, allowed to cool to room temperature, and stored for use. The samples for examination were collected and carried in sterilized bags and prepared bags. The samples included rocks covered with algae, a water sample, and a sediment sample. Under sterile environmental conditions, the samples were inoculated onto previously prepared Petri dishes containing solid growth medium by spreading either water droplets or rock particles using a loop or a glass spreader. The dishes were then placed in a cooled incubator set at 25 °C with continuous lighting at an intensity of 2500 lux. After four weeks, colonies of cyanobacteria appeared, and by the sixth week, the growth of the cyanobacteria was more pronounced.

The samples were then microscopically examined within the Petri dishes using a dissection microscope, and the colonies were marked with a marker pen. Each colony was subsequently transferred to a separate Petri dish containing fresh solid growth medium and placed back into the cooled incubator under the same conditions for the same duration, after which they were examined again to ensure the purity of the colonies. The pure isolates were then moved to a liquid growth medium in 250 mL glass flasks, each containing 100 mL of the liquid medium. These flasks were placed in a shaker incubator set to 100 rpm at 25 °C with continuous lighting at an intensity of 2500 lux.

Treatment of sewage water by nanomaterial

Wastewater treatment was performed with jar tests, the most routine method. The industrial wastewater samples were used to carry out the experiments, and the characteristics of the sample are shown in Table 1. A jar test was used to coagulate the samples using varying coagulants during the experiment. Experiments of all the coagulations were done at room temperature using 1 liter of water before the experiments were performed on the jar test. In order to prepare the samples, water was mixed with the nanomaterial mixture. The blend was placed in jars and mixed rapidly at 150 RPM for one minute with the assistance of a stirrer.After that, it was mixed slowly at 50 RPM for 20 minutes. Finally, the samples were allowed to settle for 15 minutes. Following the settling period, a floating layer of liquid was withdrawn from 5 cm below the surface of the sample for further analysis. The samples were left to stand for 24 hours and the water analyses were repeated to determine the optimal value.

Biological treatment of sewage water

The study involved treating wastewater from the hospital using batch reactors aerated by diffusers to investigate the rate of contaminant removal and determine degradation constants. Three 2-liter tanks were used as reactors, designed in a square shape to ensure complete air distribution throughout the tanks. An air compressor was employed to push air through diffusers at the bottom of the tanks, ensuring thorough mixing of the contents and achieving effective aeration with high oxygen utilization efficiency. Each tank jar measured 20 cm by 25 cm, as illustrated in Figure 1b. The tanks were sterilized, and wastewater was added after undergoing sedimentation and dilution due to high contamination levels. Then, 100 mL of each cyanobacteria species, which had already adapted to the wastewater, was inoculated into the tanks. The tanks were illuminated with the light intensity of 2500 lux for a light: dark cycle of 8:16 hours, and measurements for the study were taken at specified intervals over the course of several days.

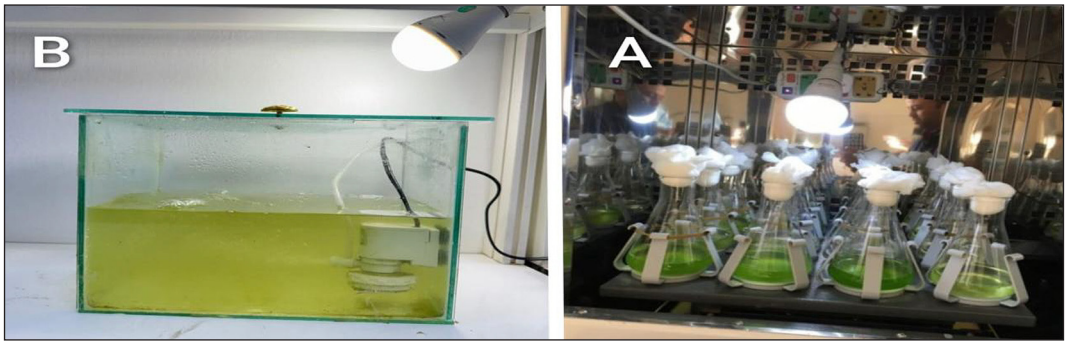

Figure 1. a) Cyanobacteria growth in the shaking incubator, b) algal growth jars

Kinetic studies

The degradation rate could be calculated by Equation 1:

$$\text{Degradation rate (\%)} = \frac{(C_0 - C_t)}{C_0} \times 100 \quad (1)$$

where: C_0 and Ct are the initial and final concentration (mg L-1), respectively.

The kinetics investigation of the uptake of

$$y = a \cdot b \cdot x/(1 + b \cdot x) \quad (2)$$

where: a – maximum adsorption or reaction capacity, b – equilibrium constant (related to the Langmuir constant Kl).

R2 (COD) coefficient of determination indicating the goodness of fit between the data and the model and reduced Chi-square – a measure of fit quality (the smaller, the better the fit).

RESULTS AND DISCUSSION

Morphological investigation of silver oxide nanoparticles

The XRD patterns of the as-synthesized Ag_2O sample are shown in Figure 2a, The XRD spectrum showed all of the diffraction peaks at 2Θ equal 32.182, 39.367, 55.93, and 77.805°, which all match the cubic phase structure and the JCPDS card number (01-076-1489) as well as the (111), (200), (200), (220), and (222) crystal planes of Ag_2O NPs of face-centered cubic (FCC), suggesting the coexistence of Ag_2O (Basha et al., 2024).

To characterize the functional groups, present in the as-prepared materials, FTIR studies were conducted. The as-synthesized Ag_2O samples' FTIR spectra were captured between 400 and 4000cm^{-1} (Figure 2b). Due to atmospheric hydration, the strong absorption peak at 2922 and 2852cm^{-1} may be attributed to the –CH stretching vibrations of the $–CH_3$ and $–CH_2$ functional groups, respectively, whereas the peak at 3429.83cm^{-1} is caused by the stretching vibration of –OH. The stretch vibrational mode of C-O-C is attributed to the peak at 1449.57 cm^{-1}, the C-O symmetric vibration to the peak at 1384.73 cm^{-1}, and the bending vibration of water (H-O-H bending) to the peak at 1640 cm^{-1}.In organic compounds, the bending vibration of the C-H bond is usually represented by the peak at 1384 cm^{-1}. A band about 600 to 750 cm^{-1} in the FTIR spectrum usually indicates the presence of Ag_2O (silver oxide). The bending vibrations of the silver-oxygen connection are linked to this band. Consequently, the existence of Ag–O is confirmed by the Ag_2O (Ag–O) bond appearing in the band at 634.69 and 634.65 cm^{-1} (Chakraborty et al., 2022).

Figure 3 displays the SEM images of the Ag_2O pristine, which reveal a quasi-spherical shape with an average size of 0.494 μm made up of tiny Ag_2O nanoparticles that are around 47 nm in size (insert). Therefore, tiny nanoparticles clumped together to form quasi-spherical particles make up the Ag_2O growth process (Pawar et al., 2015; Chakraborty et al., 2022; Basha et al., 2024). Rapid precipitation process (Equation 1) produced the pristine Ag_2O synthesis; AgOH is thermodynamically unstable, causing a breakdown that yields Ag_2O particles Equation 2.

$$AgNO_3 + NaOH \rightarrow AgOH + NaNO_3 \quad (3)$$

$$2AgOH + NaOH \rightarrow Ag_2O + H_2O \quad (4)$$

Atomic force microscopy is used to get a high-resolution imaging technique, which allows for the capture of small features to atomic scale

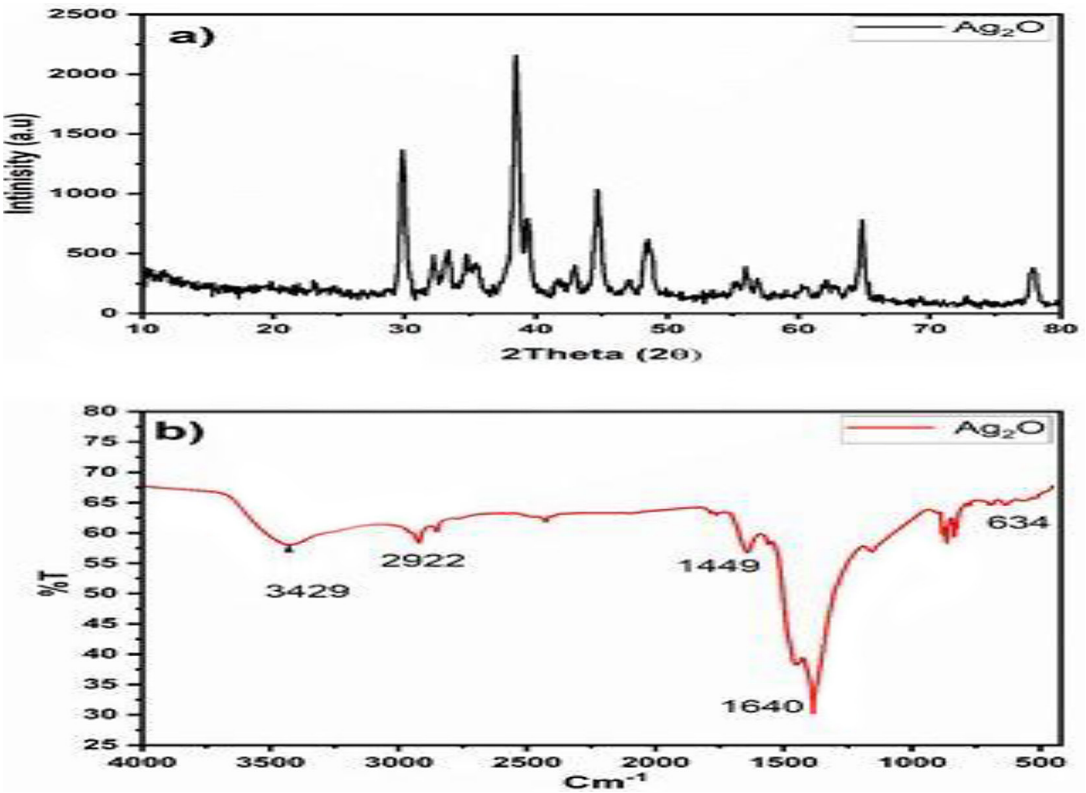

Figure 2. a) Powder X-ray diffraction pattern, b) Fourier-transform infrared spectrum of the as-synthesized Ag_2O

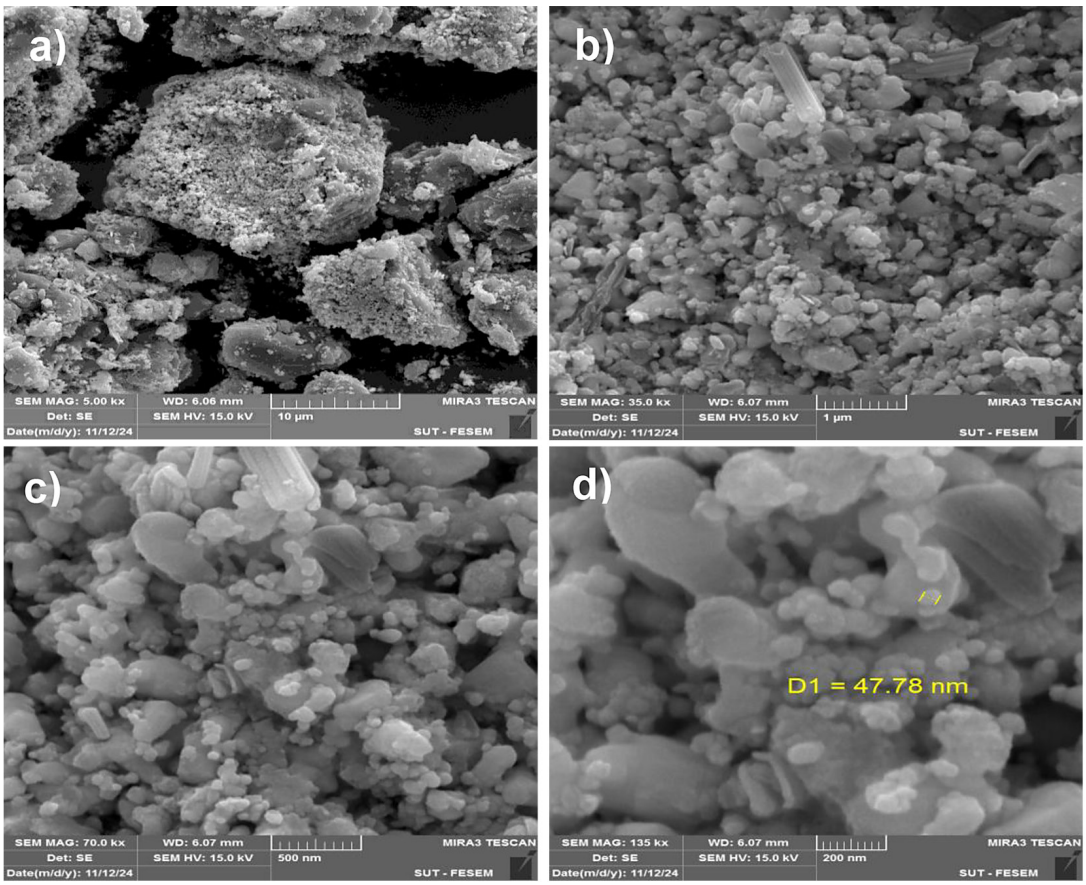

Figure 3. SEM micrographs at different magnifications: (a) to (d) represent 10 µm, 1 µm, 500 nm, and 200 nm respectively

common features in the order of the atomic lattice in real space. It is also called scanning probe microscopy. The AFM topographically maps three-dimensional features of surfaces.

The surface morphology of the synthesized Ag_2O nanoparticles was analyzed by atomic force microscopy, the surface morphology of the as-synthesized Ag_2O nanoparticles, Figure 4 (a-d) shows three-dimensional and two-dimensional atomic force micrographs of spherical shape grains with an average height of the particles equal to 9.84 nm. The RMS roughness (Sq) and grain-wise RMS roughness were equal to 2.24 nm, whereas the mean surface roughness (Sa) was equal to 1.79 nm, indicating a smooth surface. Height distribution was not highly asymmetrical with a skewness of 0.22 and a kurtosis value of 0.58, which can be referred to as a moderately smooth profile. Minimum height and maximum height were 0.00 nm and 26.52 nm, respectively, and the median height was 9.78 nm. The maximum peak height and pit depth were 16.68 nm and 9.84 nm, respectively, adding to the total height variation, Sz, of 26.52 nm. Given such a nanoscale nature, Ag_2O was considered to be a promising catalyst or sensing and energy-converting material (Figure 5).

AFM analysis of Ag_2O nanoparticles shows a distinct nanostructured morphology with a scan area of 2 × 2 µm, having a moderately rough surface with an RMS roughness (Sq) of 10.29 nm and a mean roughness (Sa) of 8.35 nm.The highest peak height (Sp) and pit depth (Sv) are 60.83 nm and 27.77 nm, respectively, so the overall height variation (Sz) is 88.60 nm. From the findings, the fundamental skewness of -0.1949 suggests that the number of depressions exceeds that of the peaks, while the kurtosis, valued at 3.641, suggests that there were more peaks, which were taller than the others, thus also deeper dips.

RESULTS AND DISCUSSION

Effect of treatment with Ag_2O

Samples of industrial wastewater from the power plant were collected and exposed to adsorption on the nanometer silver oxide surface for 24 hours, for three concentrations 50, 100, and 150 mg/l as C50, C100 and C150 respectively. While stirring and withdrawing samples every 4 hours, while placing them under the same conditions as in biological treatment, such as light and temperature (Figure 6).

The rate constant of photocatalytic degradation in a real sample. C50 has the highest b value (0.4587) compared with C100 and C150 (≈ 0.0265), indicating the strongest adsorption capacity. On the contrary, while C150 shows the highest maximum capacity ‘a’ that indicates it may hold more COD, its lower ‘b’ value reflects the weaker adsorption strength. Although strong adsorption in C50 may result in pollutant

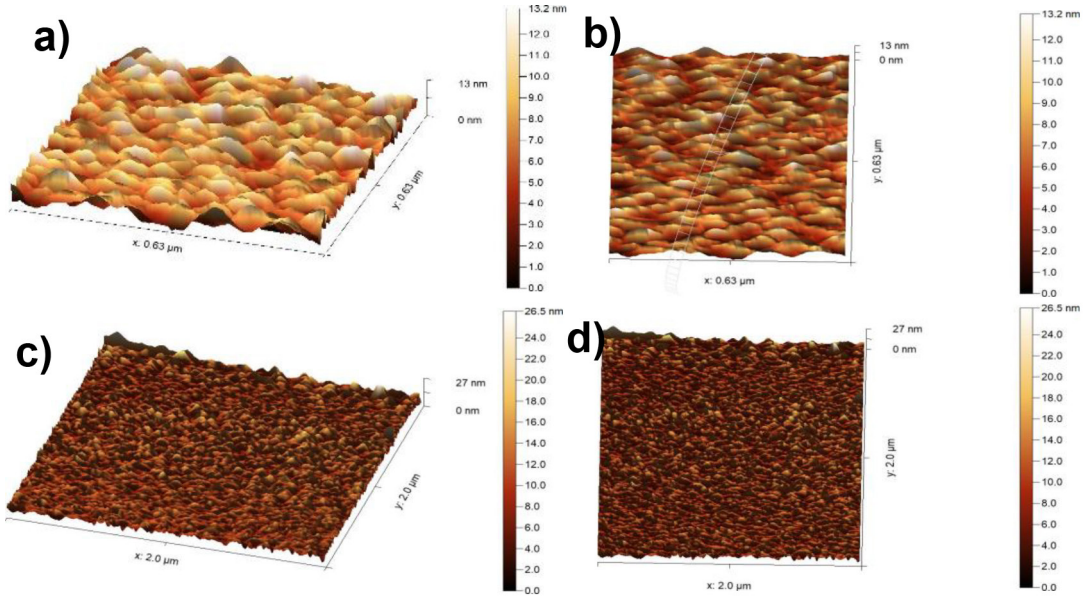

Figure 4. AFM micrographs of Ag_2O: (a, c) 3D micrographs at 0.63 µm and 2.0 µm, respectively; (b, d) 2D micrographs at 0.63 µm and 2.0 µm, respectively

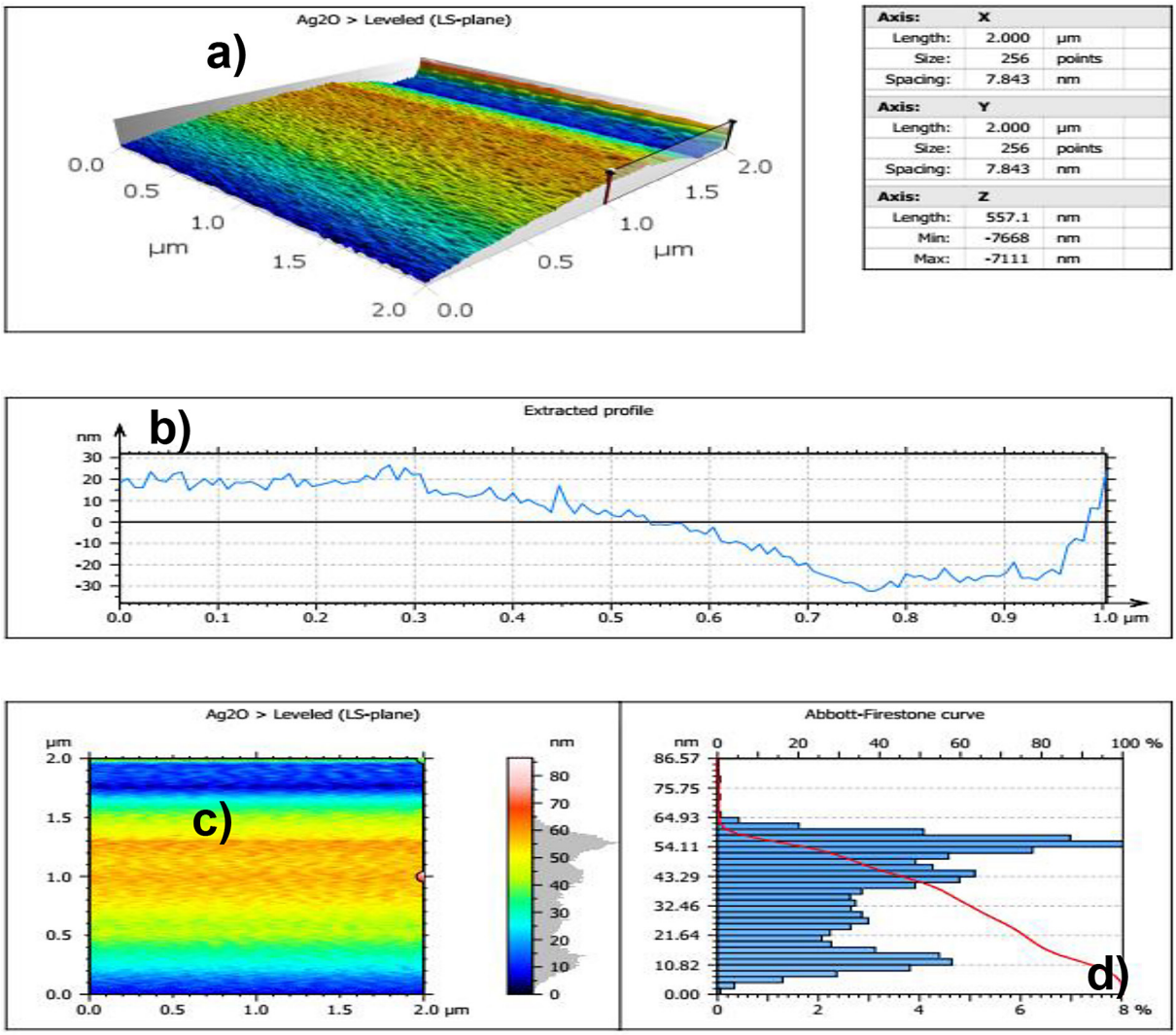

Figure 5. AFM characterization of Ag_2O nanoparticles, illustrating the surface topography and roughness parameters. (a) 3D AFM micrograph presenting the morphology of the Ag_2O sample, (b) extracted profile variations along a selected scan line, (c) 2D AFM micrograph representing height distribution with a color-coded scale. (d) Abbott-Firestone curve displaying the material volume distribution

retention without effective breakdown, making it less ideal in the case of COD degradation, C100 or C150 can be preferable owing to better balances between the adsorption strength and degradation efficiency.

Figure 7 shows the adsorption capacity of different metals (Zn, Cr, Cu, Fe, Pb) concerning time at three different concentrations of Ag_2O C50: 50 mg/L Ag_2O, C100: 100 mg/L Ag_2O, and C150: 150 mg/L Ag_2O. It was observed that with an increase in the concentration of Ag_2O, the adsorption efficiency increased for all the metals under investigation. Zn adsorption increased gradually to 75% at C150 after 24 hours, while C100 and C50 reached about 50% and 30%, respectively. About Cr adsorption, C150 showed an efficiency close to 80%, followed by C100 with ~50%, and the lowest was C50. Adsorption of Cu showed the highest removal efficiency among all studied metals: C150 reached ~96%, positioning it as the most effectively adsorbed metal, while C100 reached ~75%, and C50 below 30%. Fe adsorption showed a similar trend as Cu, where C150 exceeded 85%, C100 reached ~56%, and C150 ~27%. Among other things, the variation in Ag_2O concentration significantly changed Pb adsorption: while C150 attained ~78% removal, about 52% was reached by C100, and C50 was at 25%, further confirming that higher Ag_2O concentrations improve the performance of adsorption (Figure 8).

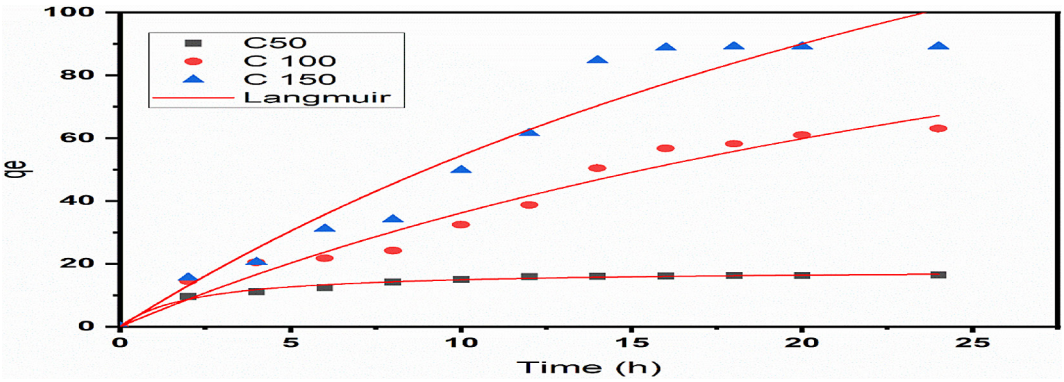

Figure 6. Adsorption kinetics of COD on Ag_2O Nps at varying concentrations

Table 1. Comparison of adsorption parameters for COD degradation

Parameter	C50	C100	C150
a (Maximum capacity)	18.1687 ± 0.3942	172.7856 ± 48.9244	260.0045 ± 97.6653
b (Equilibrium constant)	0.4587 ± 0.0515	0.0265 ± 0.0107	0.02648 ± 0.0142
R-Square (COD)	0.9892	0.9634	0.9430

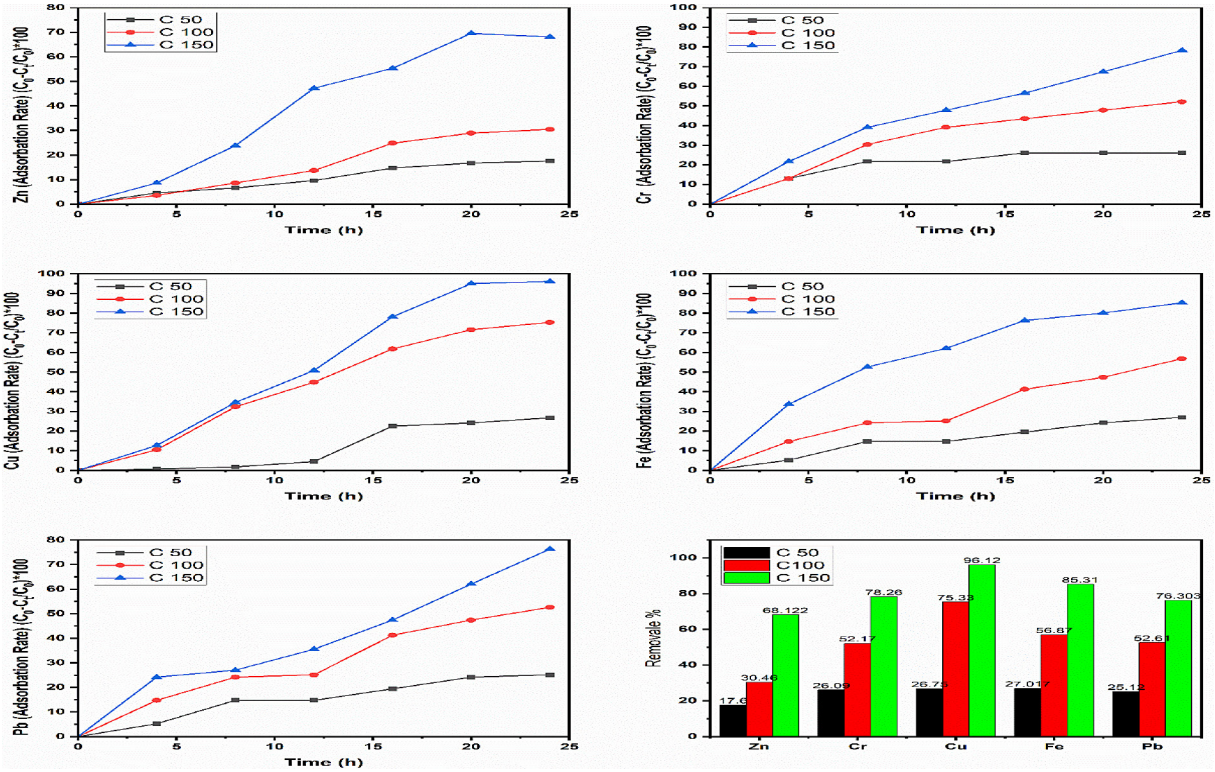

Figure 7. Adsorption efficiency of heavy metals (Zn, Cr, Cu, Fe, and Pb) over time at different Ag_2O concentrations (C50, C100, and C150)

Consequently, Ag_2O nanoparticles showed different efficiencies for various water parameters: relatively low removal of pH for all concentrations in a range from 10.42% to 27.26%, but the TDS and electrical conductivity removal increased from 34.94% to 68.65% and from 34.47% to 65.85%, respectively, reflecting increased adsorption of dissolved ionic species. The turbidity reduction is more effective, increasing from 46.62% to 91.59% with the increase in

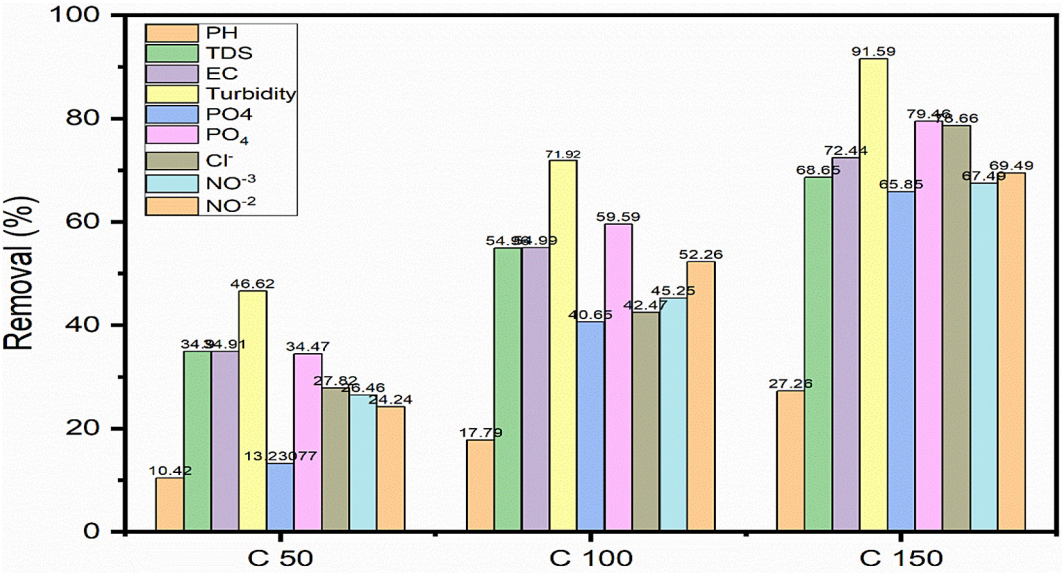

Figure 8. Removal of physicochemical parameters during treatment with Ag_2O

Ag_2O concentration. The removal of phosphate increases from 27.86% to 79.48%, showing a high adsorption affinity of the nanoparticles, which is useful in preventing eutrophication. Chloride and nitrate removal also increased, with chloride increasing from 30.77% to 67.49% and nitrate from 24.24% to 69.49%. Finally, nitrite removal increases sharply from 13.23% to 67.49%, demonstrating the potential of Ag_2O in mitigating nitrogen-based water pollutants.

Effect of biological treatment with Spirulina

Figure 9 illustrates the variations in COD measured in mg/L over time for wastewater samples treated with Spirulina from a power plant. The results cover multiple sampling dates: July 2023, October 2023, January 2024, and April 2024, with COD assessed at four intervals (D0, D5, D10, D15). Notably, the highest COD readings often occur in July 2023 (especially at D0), reflecting the raw wastewater's high pollutant concentration before treatment. Subsequent samples show a consistent downward trend in COD, particularly in January 2024 and April 2024, suggesting an additive or cumulative effect of Spirulina over time.

The concentrations of D0 COD rose, with a high reading of about 80 mg/L in July 2023. There was a considerable fall in values of post-treatment COD, with minimum values at D15 in all collection phases, bearing testimony to efficiency in Spirulina biodegradation of organic matter.

The sharp fall in COD in the review period in July 2023 bore testimony to efficiency in biotreatment with Spirulina. Conversely, in October 2023 and January 2024, a similar observation, but with relatively low values for COD at initiation, possibly a reflection of a variation in a specific period, and heightened efficiency in the treatment system. A starting value of COD (D0) in April 2024 is lesser in relation to preceding months, and a minimum value of D15 for all phases, is indicative of possibly heightened improvements in the treatment process, and heightened activity of Spirulina. There is a dramatic decline between D0 and D5, indicating the immediate effect of Spirulina on COD removal, whereas between D5 and D10, the decrease is maintained but at a bit slowed rate, indicating that a notable percentage of organic pollutants is already degraded in the first five days. At D15, COD levels are lowest during all sampling times, verifying that extended treatment duration increases wastewater cleansing. A gradual decrease in COD at various time intervals (D5, D10, D15) validates the effectiveness of Spirulina as an efficient natural bioremediation agent for wastewater treatment. This seasonal fluctuation in COD removal may be induced by some environmental parameters such as temperature, nutrient level, and growth condition of Spirulina. Initial COD (D0) values ranged from July 2023 to April 2024, showing a decrease, thus proving that continuous treatment

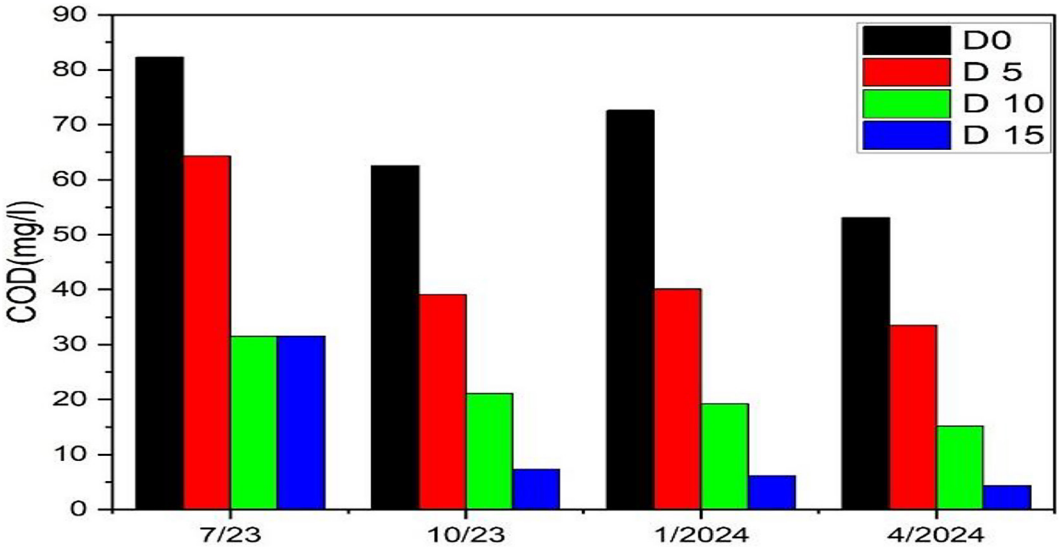

Figure 9. Variations in COD measured in mg/L across different time points (D0, D5, D10, D15) from July 2023 to April 2024

resulted in better quality wastewater overall during the duration. Its efficiency in biotreatment is patent since COD reduces progressively to over 50% within 15 days; hence, Spirulina has huge prospects in green and sustainable wastewater treatment.

Figure 10 shows the changes in water quality parameters over 15 days, measured at four-time points, including total organic substances. The parameters tested were TDS, EC, Turbidity, PO_4, SO_4, Cl^-, NO^3, and NO^{2-}, whose obtained results were normalized to their initial concentration (C/C0) for comparison. A progressive decrease in total dissolved solids and electrical conductivity could be obtained from all seasonal tests during the 15-day treatment period; however, a more significant reduction in TDS and EC during October 2023 and January 2024 thus infers optimum performance of Spirulina during cooler temperatures. Turbidity showed significant removal during all trials conducted with Spirulina, thus establishing its effectiveness in removing suspended particles. Additionally, phosphate PO_4 and sulfate SO_4 concentrations substantially declined, at times in a much cooler condition, which indicates good nutrient removal by Spirulina, its residual concentration registering minimum at D15, suggesting the continued role of bioremediation as illustrated in (Figures 10 d, e). While the chloride concentration, Cl did seem to decrease very regularly, on the slow plane of motion hence proving that Spirulina has moderated the ability to absorb chloride ions (Figure 10f).

In this study of nitrogen removal, there are significant declines visible in both the levels of NO^3 and the highest efficiency recorded in the January 2024 trial probably because of seasonal variations in metabolic activity. These reductions in turbidity were realized at D10, with great enhancements in the turbidity and nutrient levels; hence, indicating accelerated treatment efficiency. On D15, the highest drop in pollutant concentration was observed, which showed long-term effectiveness for Spirulina in wastewater remediation. Additionally, the efficiency of treatment varied with seasons: higher reductions during the cool months probably because Spirulina growth conditions were optimized. In the warmer months, the contaminant reduction rates were a little slower, likely due to higher microbial activities affecting Spirulina performance (Figure 11).

From findings Spirulina proved that able to identify heavy metal elimination for the following periods of time. By day five in this experiment, all metals were on the increase, with Cr being the most effective, at 40 to 70%, depending on the month Afterwards, it went to D10 with 70–90% of Cr being removed. During the whole period of D15, most periods gave almost 100% removal for Cr, increased for Zn and Cu, normally within 70–90%, although during April 2024, a drop was experienced. Although Spirulina proved capable of effectively removing heavy metals, particularly Cr, from wastewater, its performance varied in different months, indicating either seasonal or operational

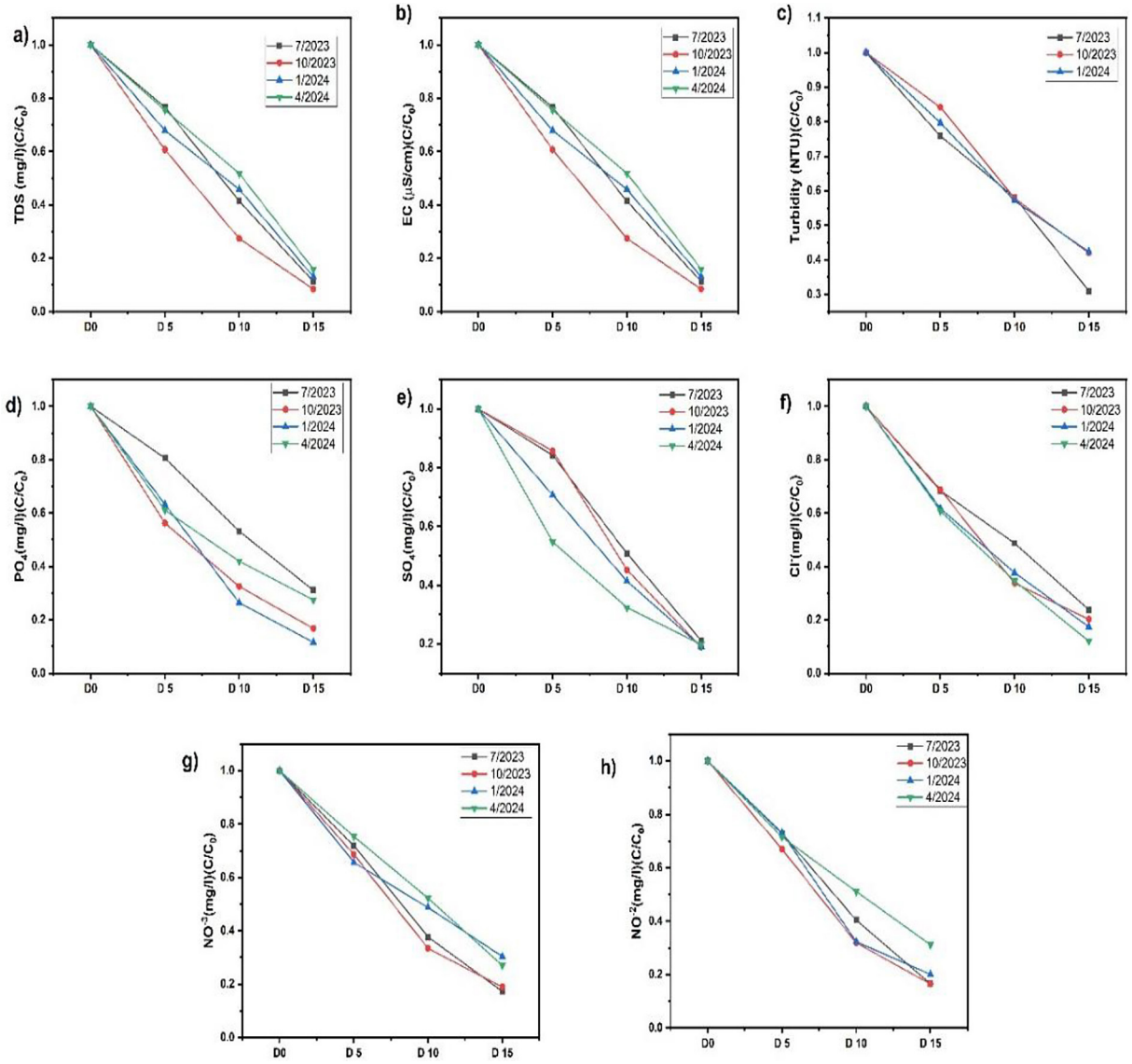

Figure 10. Changes in water quality parameters over 15 days, measured at four time points, includes total organic substances (a), electrical conductivity (b), turbidity (c), phosphate (d), sulfate (e), chloride (f), nitrate (g), and nitrous oxide (h)

factors affecting the efficiency of treatment. Overall, the results support using Spirulina for heavy metal removal as a bioremediation agent, particularly in power plant effluents.

Ag_2O nanoparticles in the present work were synthesized via a chemical precipitation method, whereby materials with particular morphological and structural characteristics have been obtained. The XRD pattern of the obtained Ag_2O indicated a cubic phase structure of the synthesized sample, whereas the diffraction peaks positioned at 2θ angle values of 32.182°, 39.367°, 55.93°, and 77.805° were assigned to the (111), (200), (220), and (222) crystal planes, respectively, corresponding to the JCPDS card number (01-076-1489). It confirms the formation of face-centered cubic Ag_2O and gives evidence of the crystallinity of the material, which is very important in catalysis and sensor technologies (Chakraborty et al., 2022). Further morphological characterization was made through SEM and revealed quasi-spherical particles with a mean diameter of approximately 0.494 µm due to the aggregation of smaller-sized nanoparticles (~ 47 nm), as obtained from (Pawar et al., 2015). The images at different magnifications revealed that these nanoparticles are reasonably well dispersed within a narrow particle size distribution signature of controlled synthesis.

To understand the functional groups, present in synthesized Ag_2O, Fourier-transform infrared

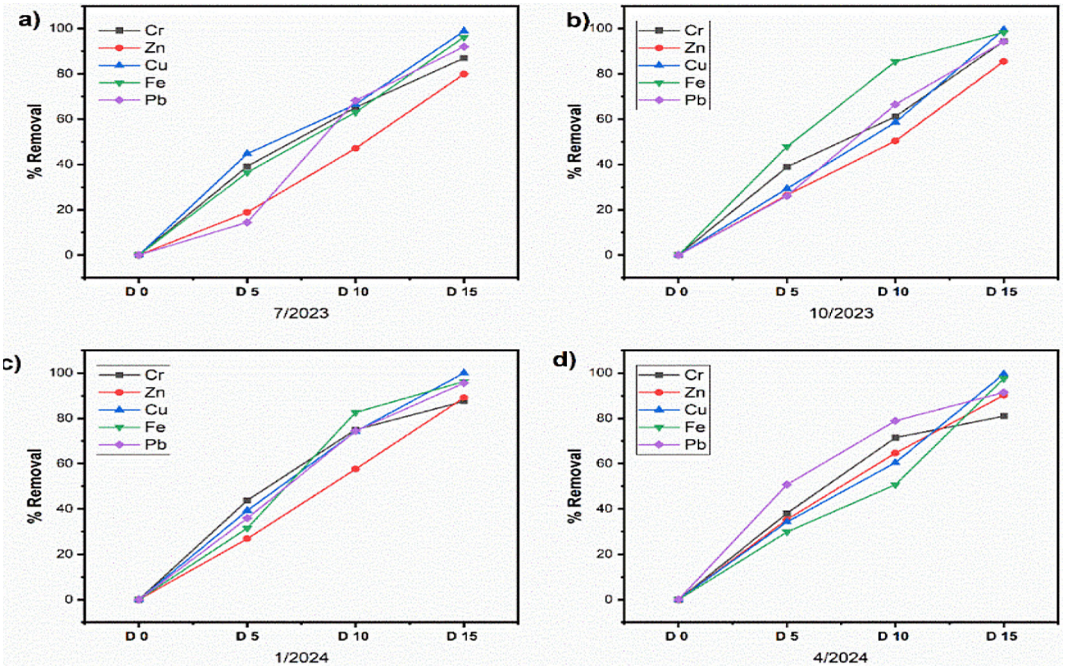

Figure 11. Removal efficiency of heavy metals from power plant wastewater using spirulina over 15 days

spectroscopy was done. FTIR spectrum of Ag_2O showed peaks at 2922 and 2852 cm^{-1}, which were attributed to the stretching frequency of –CH3 and –CH2 group, while the absorption peak at 3429.83 cm^{-1} corresponds to the –OH stretching. The peaks at 1449.57, 1384.73, and 1640 cm^{-1} indicated C-O and water molecules, while the confirmation of Ag-O bond formation was given at 634.69 and 634.65 cm^{-1}, characteristic of Ag_2O.

AFM has given high-resolution images, depicted spherical grains, and yielding an average height of 9.84 nm. The AFM analyses carried out showed that the surface topography is rather smooth, having an RMS roughness of 2.24 nm and a mean surface roughness of 1.79 nm. The distribution of height was a bit asymmetrical with a maximum height of 26.52 nm, which proved the well-defined nanostructure and showed potential application in catalysis and energy conversion. Figures 4 and 5 illustrate that AgOH precipitates fast because it is unstable thermodynamically, leading to subsequent formation of Ag_2O nanoparticles, proving the efficacy of the synthetic route adopted in the synthesis. In general, the prepared Ag_2O nanoparticles, with controlled morphology and crystallinity, possess distinctive surface properties that promise great potential in future catalysis, sensing, and energy conversion applications. Further studies are needed regarding the catalytic performance and stability of these nanoparticles in real applications.

Spirulina is a cyanobacterium, generally classified as a microalga, from which much nutrition is derived.One could realize the ample potential of spirulina regarding heavy metals removal and nutrients mainly comprising nitrogen and phosphorus through cleanup wastewater applications. Due to its high value of surface area and its adsorption-accumulation capability of heavy metals, spirulina is capable of reducing contaminants efficiently from water samples. Spirulina has also been reported in the literature to show good growth and development in wastewater while concurrently sequestering impurities there (Al-Homaidan et al., 2016). This capability allows it not only to reduce the toxicity of wastewater but also to enhance the growth and productivity of Spirulina which can be harvested as a valuable biomass. Application to the wastewater treatment processes is thus an environmentally friendly solution to improve water quality(Al-Homaidan et al., 2015; Cepoi et al., 2020; Diaconu et al., 2023).

Comparative mode of action between Ag_2O chemical treatment and Spirulina as a biotreatment

The comparative evaluation of Spirulina platensis and silver oxide (Ag_2O) nanoparticles in the treatment of real industrial wastewater demonstrated distinct mechanisms and treatment efficiencies across multiple parameters. Both

approaches showed significant reductions in contaminants, yet each displayed selectivity and variation in performance based on treatment duration, contaminant type, and mode of action.

Biological treatment using Spirulina platensis resulted in a gradual yet consistent decline in chemical oxygen demand (COD, 59.3%), nitrate (46.7%), phosphate (59.3%), turbidity (58.1%), and heavy metals such as Pb (63.4%), Cu (55.0%), and Zn (54.2%) throughout the treatment period. These findings align with those of Diaconu et al. (2023), who reported effective metal uptake by S. platensis, particularly under metal stress conditions. Furthermore, the reduction in nutrient loads agrees with observations made by Arashiro et al. (2020), who demonstrated enhanced nitrogen and phosphorus removal using Spirulina biomass in engineered systems. Seasonal influence on nutrient removal was observed, with better performance in colder temperatures. Papadopoulos et al. (2022) similarly emphasized that low temperatures favored nutrient assimilation in Arthrospira platensis due to metabolic adjustments. Additionally, Wuang et al. (2016) reported that biomass produced from aquaculture wastewater treatment with microalgae can serve as a value-added product such as biofertilizer, reinforcing the environmental and economic feasibility of this method.

Conversely, Ag_2O nanoparticles exhibited rapid removal within the first 24 hours of treatment, including COD (71.2%), turbidity (72.8%), Pb (77.5%), Cu (66.8%), Zn (69.0%), phosphate (61.4%), and nitrate (52.1%). This performance is attributed to their high oxidative activity and surface area. Chakraborty et al. (2022) confirmed the high crystallinity and catalytic potential of Ag_2O nanoparticles in organic pollutant degradation. Complementarily, Gungure et al. (2024) and Gupta et al. (2023) emphasized the strong metal adsorption capacity and fast kinetics of Ag-based nanomaterials in diverse aqueous environments. However, the stability and transformation of silver nanoparticles in wastewater must be carefully considered. Studies such as Palani et al. (2023) demonstrated that Ag nanoparticles may undergo sulfidation into Ag_2S under complex wastewater conditions, decreasing their reactivity. Similarly, Quadros and Marr (2010) raised concerns over the potential ecotoxicity and microbial inhibition caused by residual silver in aquatic systems.

Comparatively, Spirulina platensis offered a more sustainable and eco-friendly approach, suitable for long-term applications with additional biomass benefits. On the other hand, Ag_2O nanoparticles provided superior short-term performance, particularly in reducing turbidity and metal concentrations. This makes them ideal for emergency or high-load scenarios requiring quick pollutant removal.

Environmental and cost considerations

From an ecological perspective, nanoparticles might have the potential for toxicity due to residual accumulation of nanoparticles in water bodies, whereas Spirulina is fully biodegradable and contributes toward eco-friendliness. The Spirulina-based treatment is more sustainable, while nanoparticles call for careful handling and disposal. From an economic point of view, the initial cost of material synthesis and operation of nanoparticles is very high, but Spirulina is inexpensive and its operating costs are low since it uses natural growth and metabolic processes (Table 2). Spirulina is a cheaper treatment, more easily scalable, and more accessible for long-term treatment, while nanoparticles are only viable for treatments that require higher priority and faster results. The mechanisms of the treatments also vary, as in the case of silver oxide nanoparticles, it was acting directly through the oxidation of organic pollutants and adsorbed heavy metals; disruption of bacterial membranes is related to oxidative stress. In this respect, spirulina bio-accumulates and

Table 2. Comparative summary

Parameter	Silver oxide nanoparticles	Spirulina biotreatment
COD reduction	Fast (within 24 hours)	Slow but effective (15 days)
Heavy metal removal	High efficiency	Moderate efficiency
Bacterial reduction	Immediate action	Gradual reduction
pH stability	May require adjustment	Naturally stabilized
Cost	High	Low
Sustainability	Potential risks	Eco-friendly

absorbs heavy metals, enzymatically degrades organic contaminants, and exerts its natural antimicrobial action in the reduction of bacteria (Gong et al., 2021; Zhao et al., 2022).

Both methods demonstrate efficacy in wastewater treatment, with Silver Oxide nanoparticles providing rapid results and Spirulina offering a sustainable, long-term solution. The choice of method depends on treatment priorities, cost considerations, and environmental impact.

CONCLUSION

This research presents a comparative analysis of silver Ag_2O and Spirulina platensis in the remediation of real industrial wastewater. The results highlight the superior efficiency of Ag_2O in rapidly reducing COD, turbidity, and heavy metal concentrations within 24 hours, attributed to its high redox activity and nanoscale surface properties. Conversely, Spirulina achieved comparable removal rates over an extended period (15 days), offering additional benefits such as biodegradability, cost-efficiency, and environmental safety.

REFERENCES

1. Al-Homaidan, A.A., Al-Ghanayem, A.A., Al-Abbad, A.H. (2015). Adsorptive removal of cadmium ions by Spirulina platensis dry biomass. *Saudi Journal of Biological Sciences, 22*(6), 795–800. https://doi.org/10.1016/j.sjbs.2015.06.010
2. Al-Homaidan, A.A., Al-Ghanayem, A.A., Al-Abbad, A.H. (2016). Lead removal by Spirulina platensis biomass. *International Journal of Phytoremediation, 18*(2), 184–189. https://doi.org/10.1080/15226514.2015.1073673
3. Anjum, M., Al-Muhammadi, A., Shahzad, A., Khan, S., Zubair, M. (2019). Remediation of wastewater using various nano-materials. *Arabian Journal of Chemistry, 12*(8), 4897–4919. https://doi.org/10.1016/j.arabjc.2016.10.004
4. Arashiro, L.T., Montero, N., Ferrer, I., Ribeiro, R., Buttiglieri, G. (2020). Evaluation of operational conditions for nutrient removal from centrate using microalgae in an outdoor pilot-scale photobioreactor. *Journal of Environmental Management, 255*, 109891. https://doi.org/10.1016/j.jenvman.2019.109891
5. Azzi, M., Chentouf, H., Messaoudene, D., Boudiaf, L., Djerafi, R. (2024). Antimutagenic and anticoagulant therapeutic effects of Ag/Ag_2O nanoparticles from Olea europaea leaf extract: Mitigating metribuzin-induced hepato- and nephrotoxicity. *Frontiers in Pharmacology, 15*, 1485525. https://doi.org/10.3389/fphar.2024.1485525
6. Bhukal, S., Duhan, S., Ahlawat, S. (2022). Spirulina based iron oxide nanoparticles for adsorptive removal of crystal violet dye. *Topics in Catalysis, 65*(19–20), 1675–1685. https://doi.org/10.1007/s11244-022-01640-3
7. Cepoi, L., Rudi, L., Rotaru, A., Zagnat, M., Chistruga, M. (2020). Growth and heavy metals accumulation by Spirulina platensis biomass from multicomponent copper containing synthetic effluents during repeated cultivation cycles. *Ecological Engineering, 142*, 105637. https://doi.org/10.1016/j.ecoleng.2019.105637
8. Chakraborty, I., Paul, R., Pal, P. (2022). Catalytic performance of Ag_2O nanoparticles synthesized via eco-friendly precipitation method: XRD, FTIR and photocatalytic degradation studies. *Journal of Materials Research and Technology, 18*, 1305–1316. https://doi.org/10.1016/j.jmrt.2022.03.021
9. Chen, H., Pan, S.S. (2005). Bioremediation potential of Spirulina: Toxicity and biosorption studies of lead. *Journal of Zhejiang University Science B, 6*(3), 171–174. https://doi.org/10.1631/jzus.2005.B0171
10. Chen, Y.J., Chiang, Y.W., Huang, M.H. (2016). Synthesis of diverse Ag_2O crystals and their facet-dependent photocatalytic activity examination. *ACS Applied Materials & Interfaces, 8*(30), 19672–19679. https://doi.org/10.1021/acsami.6b04686
11. Diaconu, M., Mărghitaş, M., Dunca, S., Hlihor, R.M. (2023). Biosorption of heavy metals using Spirulina platensis under stress conditions: A case study. *Environmental Science and Pollution Research, 30*, 18456–18469. https://doi.org/10.1007/s11356-022-24963-0
12. El Messaoudi, N., Elhalil, A., Zouahri, A., Elghoul, Y., El Alem, N. (2022). Green synthesis of Ag_2O nanoparticles using *Punica granatum* leaf extract for sulfamethoxazole antibiotic adsorption: Characterization, experimental study, modeling, and DFT calculation. *Environmental Science and Pollution Research*, 30(34), 81352–81369. https://doi.org/10.1007/s11356-022-21554-7
13. El-Nashar, W. Y. (2017). Effect of drains coverings on environment by using value engineering. *Alexandria Engineering Journal*, 56(3), 327–332. https://doi.org/10.1016/j.aej.2017.05.013
14. Fayyadh, A. A., Alzubaidy, M. H. J. (2021). Green-synthesis of Ag_2O nanoparticles for antimicrobial assays. *Journal of the Mechanical Behavior of Materials*, *30*(1), 228–236. https://doi.org/10.1515/jmbm-2021-0024
15. Gaur, K., Bhatt, D., Rawat, M., Arya, D., Pandey, A. (2024). Exploring the nutritional and medicinal potential of *Spirulina*. *Natural Resources for Human*

Health, *4*(3), 277–286. https://doi.org/10.53365/nrfhh/188021

16. Gong, Y., Zheng, X., Huang, J. (2021). *Chlorella sp.* Mg shows special trophic transitions and biomass production. *Bioresource Technology Reports*, *16*, 100854. https://doi.org/10.1016/j.biteb.2021.100854
17. Gudkov, S. V., Kistenev, Y. V., Zubarev, I. V., Golubev, A. I. (2022). Ag_2O nanoparticles as a candidate for antimicrobial compounds of the new generation. *Pharmaceuticals*, *15*(8), 968. https://doi.org/10.3390/ph15080968
18. Gungure, E., Yılmaz, B., Sürer, M. G. (2024). Application of silver-based nanomaterials for metal ion removal in wastewater: A review of mechanisms and effectiveness. *Journal of Environmental Chemical Engineering*, *12*(1), 110298. https://doi.org/10.1016/j.jece.2023.110298
19. Gupta, S., Kumar, A., Sharma, P. (2023). Rapid adsorption of toxic heavy metals by silver oxide nanoparticles synthesized using green methods. *Journal of Water Process Engineering*, *51*, 103254. https://doi.org/10.1016/j.jwpe.2023.103254
20. Hirata, T., Tanaka, M., Ooike, M., Tsunomura, T., Sakaguchi, M. (2000). Antioxidant activities of phycocyanobilin prepared from *Spirulina platensis*. *Journal of Applied Phycology*, *12*(3–5), 435–439. https://doi.org/10.1023/A:1008175217194
21. Karkos, P. D., Leong, S. C., Karkos, C. D., Sivaji, N., Assimakopoulos, D. A. (2010). *Spirulina* in clinical practice: Evidence-based human applications. *Evidence-Based Complementary and Alternative Medicine*, 2011, 531053. https://doi.org/10.1093/ecam/nen058
22. Karthik, P., Karuthapandi, M., Suganthi, S., Rajalakshmi, M., Arumugam, A. (2023). Effective photodegradation of organic water pollutants by the facile synthesis of Ag_2O nanoparticles. *Surfaces and Interfaces*, *40*, 103088. https://doi.org/10.1016/j.surfin.2023.103088
23. Kato, S., Kansha, Y. (2024). Comprehensive review of industrial wastewater treatment techniques. *Environmental Science and Pollution Research*, *31*(39), 51064–51097. https://doi.org/10.1007/s11356-024-34584-0
24. Kurtulus, R., Gökçe, H. S., Bilgin, V., Altındal, Ş. (2021). A comprehensive examination of zinc-boro-vanadate glass reinforced with Ag_2O in physical, optical, mechanical, and radiation shielding aspects. *Applied Physics A: Materials Science and Processing*, *127*(2). https://doi.org/10.1007/s00339-021-04282-6
25. Lu, P., Zhao, Z., Liu, D., Li, D. (2016). New insight into advection of organic contaminate plume at drain outlet areas. *Environmental Nanotechnology, Monitoring and Management*, *6*, 76–82. https://doi.org/10.1016/j.enmm.2016.08.001
26. Najam, A., Papa, M., Taiyab, N. (2014). United Nations Environment Programme. In *Essential Concepts of Global Environmental Governance* 245–247. https://doi.org/10.4324/9780203553565-104
27. Nishat, A., Ali, H., Rahman, M. T., Haque, S. (2023). Wastewater treatment: A short assessment on available techniques. *Alexandria Engineering Journal*, *76*, 505–516. https://doi.org/10.1016/j.aej.2023.06.054
28. Obaideen, K., Altarawneh, M., Al-Gheethi, A. A., El Hanandeh, A. (2022). The role of wastewater treatment in achieving sustainable development goals (SDGs) and sustainability guideline. *Energy Nexus*, *7*, 100112. https://doi.org/10.1016/j.nexus.2022.100112
29. Palani, S., Arumugam, K., Senthilkumar, M. (2023). Stability and sulfidation behavior of silver nanoparticles in wastewater treatment systems. *Environmental Nanotechnology, Monitoring & Management*, *20*, 100669. https://doi.org/10.1016/j.enmm.2023.100669
30. Papadopoulos, K. I., Kountouriotis, V., Tzovenis, I. (2022). Temperature-dependent nutrient assimilation in *Arthrospira (Spirulina) platensis*: Implications for outdoor cultivation. *Bioresource Technology Reports*, *19*, 101134. https://doi.org/10.1016/j.biteb.2022.101134
31. Pawar, O., Deshpande, N., Dagade, S., Waghmode, S., Nigam Joshi, P. (2015). Green synthesis of silver nanoparticles from purple acid phosphatase apoenzyme isolated from a new source *Limonia acidissima*. *Journal of Experimental Nanoscience*, *11*(1), 28–37. https://doi.org/10.1080/17458080.2015.1025300
32. Pedrosa, M., Almeida, A. R., Tavares, D. S., Valente, A. J. M., Santos, J. V. (2022). *Spirulina*-based carbon bio-sorbent for the efficient removal of metoprolol, diclofenac and other micropollutants from wastewater. *Environmental Nanotechnology, Monitoring & Management*, *18*, 100720. https://doi.org/10.1016/j.enmm.2022.100720
33. Quadros, M. E., Marr, L. C. (2010). Environmental and human health risks of aerosolized silver nanoparticles. *Journal of the Air & Waste Management Association*, *60*(7), 770–781. https://doi.org/10.3155/1047-3289.60.7.770
34. Rai, M., Yadav, A., Gade, A. (2009). Silver nanoparticles as a new generation of antimicrobials. *Biotechnology Advances*, *27*(1), 76–83. https://doi.org/10.1016/j.biotechadv.2008.09.002
35. Basha S.K., Arunachalam, K., Lakshmanan, A., Ahamed, M.R. (2024). Facile synthesis of silver nanoparticles from sustainable *Sargassum* sp. seaweed material and its anti-inflammatory application.

Cureus, *16*(4), e57754. https://doi.org/10.7759/cureus.57754

36. APHA, AWWA, WEF. (2017). *Standard Methods for the Examination of Water and Wastewater* (23rd ed.). Washington, DC: American Public Health Association.
37. Thennarasu, G., Rajeswari, R., Prabu, P., Kumar, P. S. (2024). A comprehensive review on the application of semiconductor nanometal oxides photocatalyst for the treatment of wastewater. *Clean Technologies and Environmental Policy*. https://doi.org/10.1007/s10098-024-02960-6
38. Waterbury, J. B. (2006). The Cyanobacteria – solation, purification and identification. In *The Prokaryotes* 1053–1073. https://doi.org/10.1007/0-387-30744-3_38
39. Wuang, S. C., Khin, M. C., Lin, C. C. (2016). Use of microalgae for removing nutrients from aquaculture wastewater and its biomass utilization for producing biofertilizer. *Bioresource Technology*, *216*, 579–586. https://doi.org/10.1016/j.biortech.2016.05.106
40. Yashavanth, P. R., Das, M., Maiti, S. K. (2021). Recent progress and challenges in cyanobacterial autotrophic production of polyhydroxybutyrate (PHB), a bioplastic. *Journal of Environmental Chemical Engineering*, *9*(4), 105379. https://doi.org/10.1016/j.jece.2021.105379
41. Zhao, Q., Wang, Z., Liu, C., Liu, Y., Zhou, Y. (2022). Efficient treatment of phenol wastewater by co-culture of *Chlorella vulgaris* and *Candida tropicalis*. *Algal Research*, *65*, 102738. https://doi.org/10.1016/j.algal.2022.102738